


Article

Self-Assembly by Tridentate or Bidentate Ligand: Synthesis and Vapor Adsorption Properties of Cu(II), Zn(II), Hg(II) and Cd(II) Complexes Derived from a Bis(pyridylhydrazone) Compound

Hong-Juan Liu, Rui Yi, Dong-Mei Chen, Chao Huang *  and Bi-Xue Zhu *

Key Laboratory of Macrocyclic and Supramolecular Chemistry of Guizhou Province, Guizhou University, Guiyang 550025, China; hjlju0323@163.com (H.-J.L.); lujhgzu@163.com (R.Y.); chendm3807@163.com (D.-M.C.)

* Correspondence: chuang1@gzu.edu.cn (C.H.); bxzhu@gzu.edu.cn (B.-X.Z.)

Abstract: Four complexes, $[\text{Cu}_4\text{L}_2(\text{OCH}_3)_2(\text{CH}_3\text{OH})_2]\cdot 2\text{H}_2\text{O}$ (**1**), $[\text{Zn}_2\text{L}_2\text{Cl}_4]\cdot 2\text{H}_2\text{O}\cdot 2\text{CH}_3\text{OH}$ (**2**), $[\text{Hg}_2\text{L}_2\text{Br}_4]\cdot 4\text{CH}_3\text{OH}$ (**3**), and $\{[\text{CdL}_2\text{Cl}_2]\cdot 4\text{H}_2\text{O}\cdot 4\text{CH}_3\text{OH}\}_n$ (**4**), have been synthesized and characterized from a bis(pyridylhydrazone) ligand (**L**) with copper(II), zinc(II), mercury(II) or cadmium(II), respectively. Complex **1** exists as a centrosymmetric tetranuclear dimer with **L** as deprotonated tridentate ligand. Complexes **2** and **3** exist as centrosymmetric metallamacrocycles with **L** as bidentate ligand. Complex **4** exists as a 1D looped-chain coordination polymer. The thermal stabilities and vapor adsorption properties of the four complexes were investigated as well.

Keywords: pyridylhydrazone; complex; crystal structure; vapor adsorption



Citation: Liu, H.-J.; Yi, R.; Chen, D.-M.; Huang, C.; Zhu, B.-X. Self-Assembly by Tridentate or Bidentate Ligand: Synthesis and Vapor Adsorption Properties of Cu(II), Zn(II), Hg(II) and Cd(II) Complexes Derived from a Bis(pyridylhydrazone) Compound. *Molecules* **2021**, *26*, 109. <https://doi.org/10.3390/molecules26010109>

Received: 16 November 2020

Accepted: 22 December 2020

Published: 29 December 2020

Publisher's Note: MDPI stays neutral with regard to jurisdictional claims in published maps and institutional affiliations.



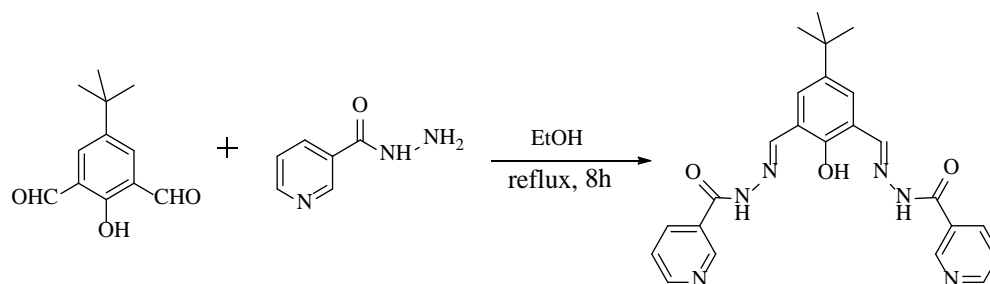
Copyright: © 2020 by the authors. Licensee MDPI, Basel, Switzerland. This article is an open access article distributed under the terms and conditions of the Creative Commons Attribution (CC BY) license (<https://creativecommons.org/licenses/by/4.0/>).

1. Introduction

Within the field of supramolecular chemistry, hydrazone derivatives have been one of the most important classes of flexible and versatile polydentate ligands which show very high efficiency in chelating with transition metal ions [1–6]. The coordinating ability of hydrazones is possible due to the nucleophilic character of the nitrogen atoms of the triatomic structure C=N-N of the azomethine group [7,8]. So far, hydrazone-based metal complexes have received considerable attention from chemists in many applications such as chromogenic reagents in the spectrophotometric determination of transition-metal ions, metal extracts and biologically active compounds [9]. They have also been demonstrated to possess diverse pharmacological properties [10–17], catalytic properties [18,19], adsorption properties [20,21], electrochemical properties [22], luminescent properties [23,24], etc.

Pyridyl moiety is probably the most popular building block for the construction of metal-organic networks due to its strong coordination ability to metal ions [25–27]. In recent years, bis(pyridylhydrazone) ligands are often used in the construction of novel supramolecular architectures and promising candidates for metallo-anion receptors. Coordination polymers with organic ligands based on dipyridylamide moieties reveal that dipyridyl groups are a good choice for connecting metal centers and the hydrogen bonding of amide functionality can add extra dimensionality to the resulting structures. Several beautiful examples have been reported recently and further demonstrate the potential in the organization of the primary molecules in the solid state [28–31].

In this work, a bis(pyridylhydrazone) ligand (**L**) was synthesized by the Schiff base condensation reaction of 5-(tert-butyl)-2-hydroxyisophthalaldehyde with nicotinic hydrazide (Scheme 1). Four complexes have been synthesized and characterized from the bis(pyridylhydrazone) ligand with Cu(II), Zn(II), Hg(II), and Cd(II), respectively. The different geometries of the complexes disclose that the coordination sites play important roles in the formation of different structures.



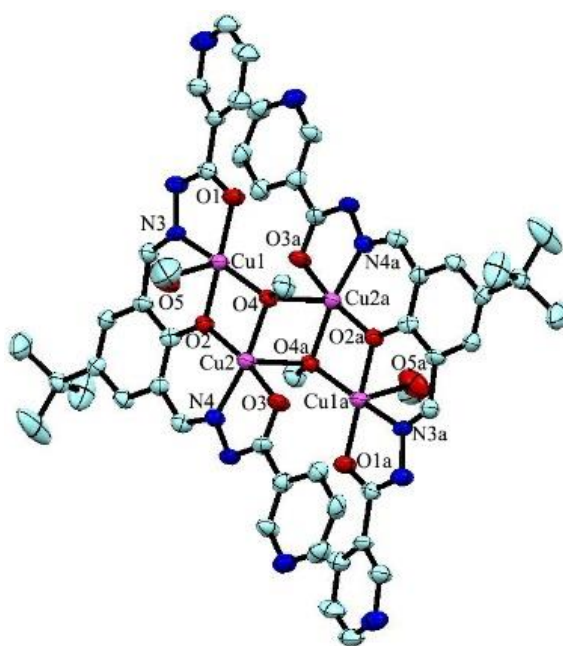
Scheme 1. Synthesis of the bis(pyridylhydrazone) Schiff base ligand.

2. Results and Discussion

2.1. Description of Crystal Structures

2.1.1. Crystal Structure of Complex 1

The reaction between the ligand and $\text{Cu}(\text{Ac})_2$ yielded green crystals of tetranuclear $[\text{Cu}_4\text{L}_2(\text{OCH}_3)_2(\text{CH}_3\text{OH})_2]\cdot 2\text{H}_2\text{O}$ (**1**). Complex **1** crystallizes in the triclinic space group $P\bar{1}$. In the complex, the Addison τ_5 parameters of copper(II) are 0.09 and 0 for Cu1 and Cu2 ($\tau_5 = 0$ for a perfectly square-pyramidal geometry, and $\tau_5 = 1$ for a perfectly trigonal-bipyramidal geometry) [32], suggesting that both copper atoms adopt a square-pyramidal geometry (Figure 1a). The structure can be considered as a centrosymmetric tetranuclear dimer complex which consists of two trianionic ligands, two methanol molecules, two methoxide ions, and four copper(II) ions. The copper atom is coordinated with three oxygen atoms and one nitrogen atom in the basal positions, and a methanol oxygen atom (for Cu1) or a methoxide oxygen atom (for Cu2) in the axial position. In the molecule, the Cu1-Cu2 distance is 2.957(4) Å, which is consistent with similar complexes found in the literature [33,34]. Noticeably, $[\text{Cu}_2(\mu_3\text{-OCH}_3)_2\text{Cu}_2\text{a}]$ forms a square with Cu2-Cu2a separation of 2.973(5) Å and the distance of the two μ_3 -methoxide oxygen atoms bridged by Cu2/Cu2a is 2.969(4) Å, which is well comparable with previously reported copper complexes [35]. The packing view shows O–H \cdots N hydrogen bonds between two neighboring ligands constitute an infinite 1D supramolecular chain (Figure 1b).



(a)

Figure 1. Cont.

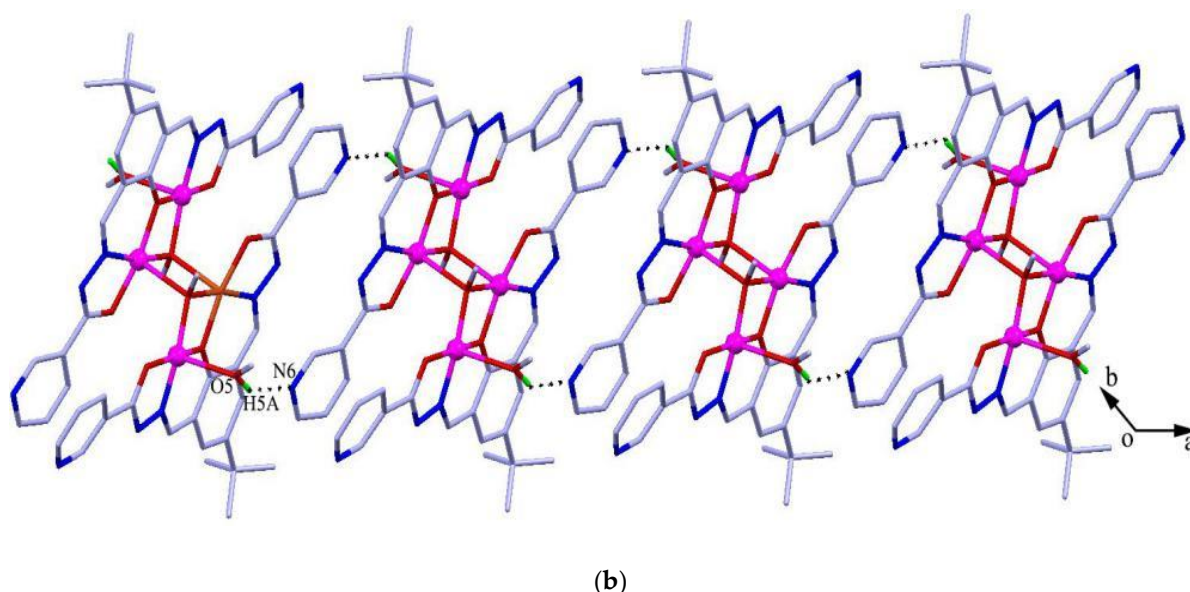


Figure 1. (a) Molecular structures of **1** with anisotropic displacement ellipsoids drawn at the 50% probability level, and (b) 1D structure formed by O–H···N hydrogen bonds. Symmetry code: (a) $1 - x, 1 - y, 1 - z$.

2.1.2. Crystal Structure of Complexes **2** and **3**

The reaction of the ligand with ZnCl_2 or HgBr_2 in the MeOH–DMF solution gave the complex $[\text{Zn}_2\text{L}_2\text{Cl}_4] \cdot 2\text{H}_2\text{O} \cdot 2\text{CH}_3\text{OH}$ (**2**) or $[\text{Hg}_2\text{L}_2\text{Br}_4] \cdot 4\text{CH}_3\text{OH}$ (**3**) as colorless block crystals. Both of the two complexes crystallize in triclinic space group $P\bar{1}$. Complexes **2** and **3** are isostructural except for the variation in the lattice solvent molecules, and they exist with very similar coordination configurations. Therefore, only the crystal structure of complex **2** is discussed herein. Complex **2** exists as a centrosymmetric 36-membered binuclear metallamacrocycle, which is composed of two Zn(II) ions, two ligands, four Cl anions, two methanol and two H_2O molecules. Each Zn(II) is four-coordinated by two Cl anions and two pyridyl nitrogen atoms with a slightly distorted tetrahedral geometry deduced by its structural parameter $\tau_4 = 0.91$ ($\tau_4 = 0$ for a perfectly a square-planar geometry, and $\tau_4 = 1$ for a perfectly tetrahedral geometry) [36]. The Zn1–N1, Zn1–N6a, Zn1–Cl1 and Zn1–Cl2 bond lengths are 2.079(3), 2.060(3), 2.2264(16) and 2.2070(16) Å, respectively. The N–Zn–Cl bond angles are in the range of $104.46(8)^\circ \sim 108.21(9)^\circ$. The bond angles for Cl1–Zn–Cl2 and N1–Zn–N6a are $123.80(5)^\circ$ and $104.21(12)^\circ$, respectively, which are consistent with those found in the similar complexes [37]. The dihedral angles between the pyridyl and the central benzene ring, and the neighboring pyridyl ring are 30.45° and 76.48° , respectively. The dinuclear structures connect to each other through N2–H2A···O3 hydrogen bond interactions to form 1D channels in the overall three dimensional network (Figure 2b).

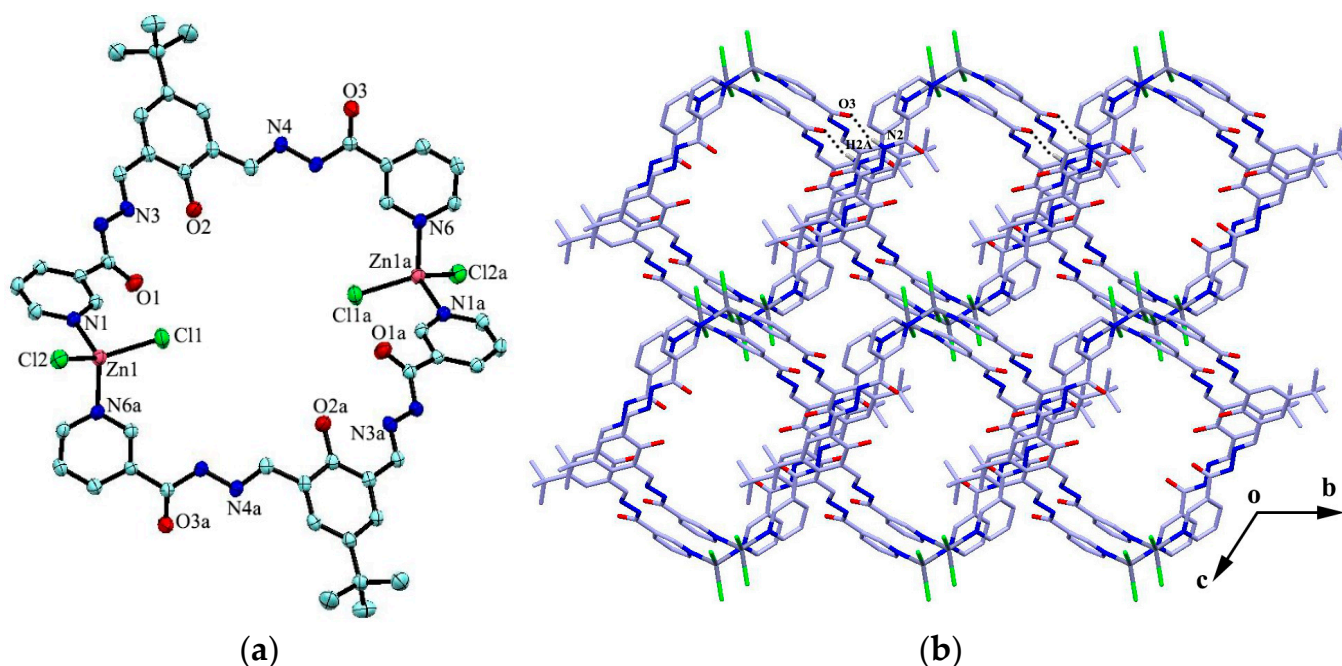


Figure 2. (a) Molecular structures of **2** with anisotropic displacement ellipsoids drawn at the 50% probability level and (b) 3D network formed through intermolecular hydrogen bonds (Some hydrogen atoms are omitted for clarity). Symmetry code: (a) $1 - x, 2 - y, 1 - z$.

2.1.3. Crystal Structure of Complex 4

The reaction of the ligand and CdCl_2 in MeOH-DMF (4:1, V/V) gave the complex $\{[\text{CdL}_2\text{Cl}_2] \cdot 4\text{H}_2\text{O} \cdot 4\text{CH}_3\text{OH}\}_n$ (**4**) as yellow block crystals. Complex **4** crystallizes in the triclinic space group $P\bar{1}$. The cadmium atom is six-coordinated by two chlorine atoms and four pyridyl nitrogen atoms from four adjacent ligands in a slightly distorted octahedral geometry. The four pyridyl nitrogen atoms constitute the basal plane of the octahedron, and the two chlorine atoms are located at the axial positions (Figure 3a). The ligands act as bidentate building blocks by pyridyl nitrogen atoms, linking the $\text{Cd}(\text{II})$ ions to form a 1D looped-chain of 36-membered macrocycles propagating along the c axis with the $\text{Cd} \cdots \text{Cd}$ distance of 16.68 Å. Each macrocycle is found to be associated with four methanol molecules via $\text{O-H} \cdots \text{O}$, $\text{N-H} \cdots \text{O}$ or $\text{O-H} \cdots \text{Cl}$ hydrogen bonds ($\text{D} \cdots \text{A} = 2.726(10) - 3.112(4)$ Å). Intermolecular hydrogen bonding interactions ($\text{N2-H2A} \cdots \text{O3}$) and $\pi \cdots \pi$ stacking interactions between the adjacent benzene rings (the centroid-to-centroid distance is 3.912 Å) are formed to generate a 2D framework along the bc plane (Figure 3b), which is further linked by $\text{C22-H22} \cdots \text{Cl1}$ hydrogen bond interactions, resulting in a 3D porous supramolecular network (Figure 3c).

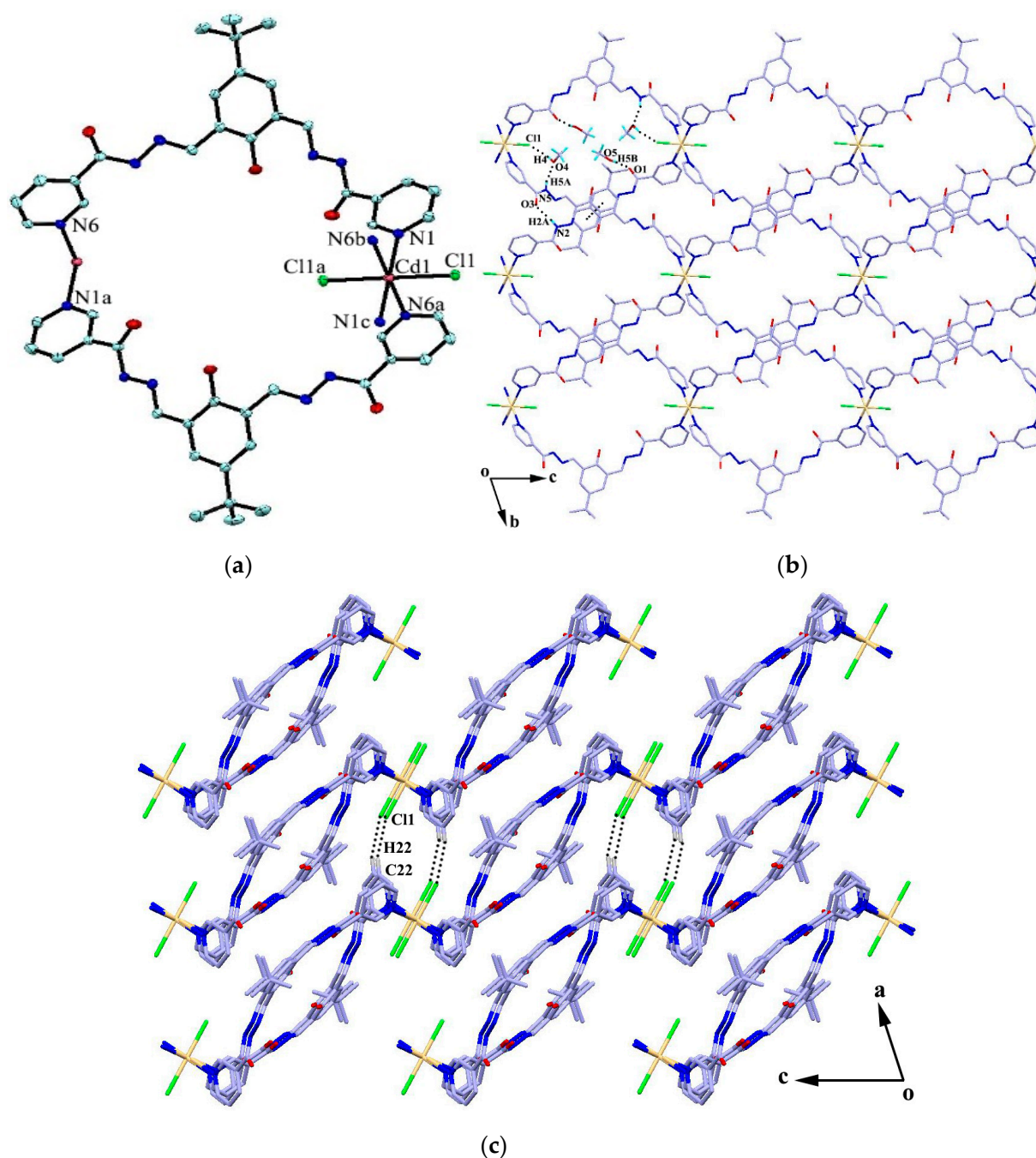


Figure 3. (a) Coordination environment of the Cd atom in complex 4; (b) 2D framework formed by hydrogen bonds and $\pi \cdots \pi$ stacking interactions; and (c) 3D porous supramolecular network. Symmetry codes: (a) $1 - x, -y, 1 - z$; (b) $-1 + x, y, 1 + z$; and (c) $-x, -y, 2 - z$.

2.1.4. Structural Comparison

The organic ligands and metal ions play important roles in the formation of the final coordination frameworks and topologies. As described above, self-assembly of the ligands with Cu(II), Zn(II), Hg(II), and Cd(II) lead to 0D or 1D structures, which are all obtained in similar solvent evaporation conditions (MeOH/DMF). The structural analysis reveals that each copper(II) ion is five-coordinated with a square-pyramidal geometry. The zinc(II) and mercury(II) ions are four-coordinated with a slightly distorted tetrahedral geometry, and the cadmium ion is six-coordinated with a distorted octahedral geometry. Besides, it was found that the bis(pyridylhydrazone) compound acts as a tridentate deprotonated

ligand in complex 1, while as a bidentate ligand in complexes 2–4. In short, the diversity of coordination preferences of metal ions as well as the nature of the ligands affect the assembly of the architectures.

2.2. TG Analyses of the Complexes

Thermal stabilities of the four complexes were measured by thermogravimetric analysis (TGA) between 25 and 800 °C in the N₂ atmosphere at the heating rate of 10 °C min⁻¹ (Figure 4). Complex 1 shows a slight weight loss from room temperature to 200 °C corresponding to the release of two H₂O molecules (observed weight loss 2.7%, calculated 2.8%). The complex began to decompose from about 200 °C due to the release of the methanol molecules and methoxide ion, as well as the decomposition of the organic frameworks. For complex 2, there is a weight loss (5.2%) in the range of 25 to 140 °C, which is attributed to the loss of solvent molecules (calculated 8.6%). The organic framework begins to decompose at above 400 °C. Complex 3 shows a continuous weight loss (9.6%) in the temperature range of 25 to 240 °C, which is due to the loss of methanol molecules (calculated 10.1%). The complex begins to decompose at above 250 °C with a sharp weight loss, which is accompanied by the elimination of HgBr₂. Complex 4 exhibits a slight weight loss (6.6%) in the temperature range 25 to 290 °C, then begins to decompose the organic frameworks with a sharp weight loss. The results show that the solvent molecules can affect the thermal stability of the complexes.

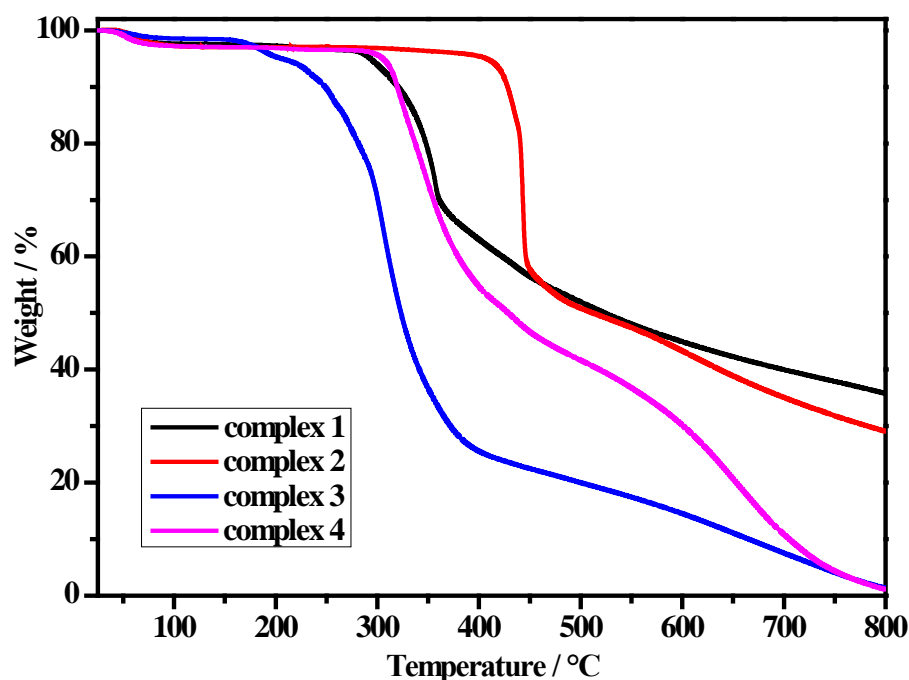


Figure 4. TGA curves for complexes 1–4.

2.3. Adsorption Measurements of the Complexes

Considering different hydrogen bond interactions and porous structures in the complexes, we explored methanol vapor adsorption for the four complexes at room temperature (Figure 5). The samples activation occurred at 353 K in a dynamic vacuum for 8 h until the outgas rate was less than 4 mmHg·min⁻¹. Vapor adsorption isotherms were obtained by a Micromeritics ASAP 2020 system under the methanol vapor atmosphere. The Langmuir surface area and BET (Brunauer–Emmett–Teller) surface area for complexes 1–4 are listed in Table 1. As shown in Figure 5, the adsorption isotherms show a typical type III nature with the largest quantity adsorbed for complexes 1–4 are 7.81, 5.59, 6.36 and 6.72 mmol·g⁻¹, which are similar to the complexes reported in previous references [38,39]. It is meaningful for the complexes to be potential materials as adsorbent of methanol vapor.

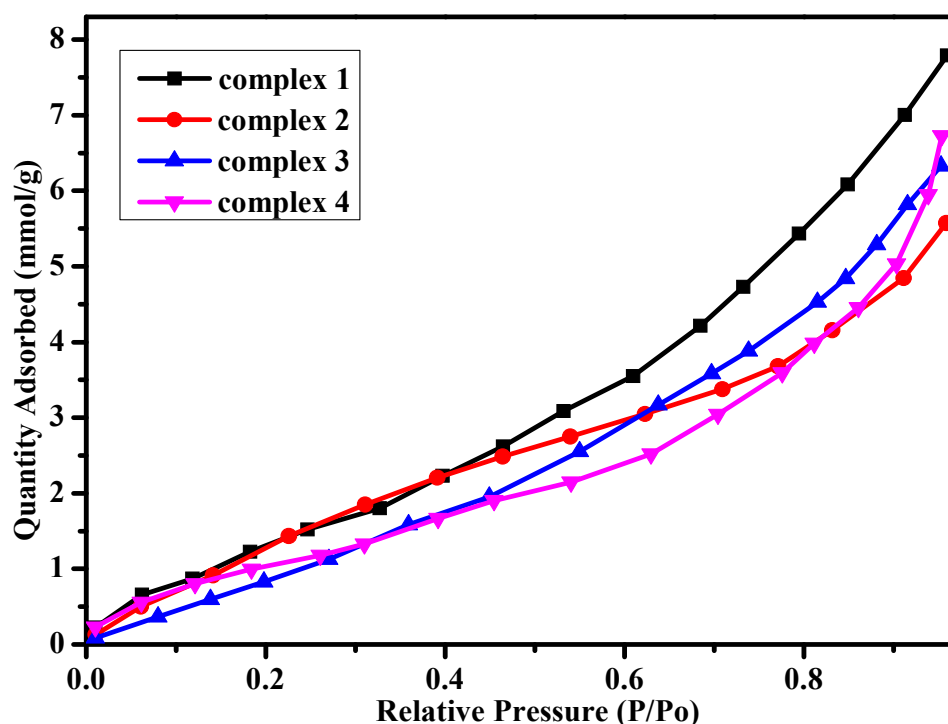


Figure 5. Methanol vapor adsorption for complexes 1–4 at 298 K.

Table 1. Langmuir and BET (Brunauer–Emmett–Teller) surface area for complexes 1–4.

Complex	1	2	3	4
Langmuir surface area (m ² /g)	687	398	489	496
BET surface area (m ² /g)	585	309	355	372

3. Experimental Section

3.1. Materials and Physical Measurements

All reagents and solvents were commercially available (Aladdin, Shanghai, China) and used without further purification. Melting points (uncorrected) were determined by an LTD 9100 apparatus (Electrothermal Engineering, London, UK). ¹H NMR spectra were recorded in DMSO-*d*₆ using a JNM-ECZ 400 MHz NMR spectrometer (JEOL, Tokyo, Japan). IR spectra were recorded on a VERTEX 70 FTIR instrument (Bruker, Germany) with KBr pellets in the range of 4000–400 cm^{−1} regions. Elemental analysis (C,H,N) were carried out on a Vario ELIII elemental analyzer (Elementar, Berlin, Germany). The crystal diffraction data were collected with a D8 VENTURE diffractometer (Bruker, Berlin, Germany). Thermogravimetric analysis (TGA) curves were carried out on a TGA-7 thermal analyzer (Perkin Elmer, Waltham, MA, USA) in the temperature region of 25–800 °C. The vapor adsorption measurements of methanol were performed by an ASAP 2020 (Micrometrics, Norcross, GA, USA) outfitted with a turbo molecular drag pump.

3.2. Synthesis

3.2.1. Synthesis of the Ligand

5-(*tert*-butyl)-2-hydroxy-isophthalaldehyde was synthesized according to previous literature [40]. A solution of 5-(*tert*-butyl)-2-hydroxy-isophthalaldehyde (0.42 g, 2.0 mmol) in anhydrous ethanol (50 mL) was heated and stirred until dissolved, and nicotinic hydrazide (0.55 g, 4.0 mmol) in anhydrous ethanol (50 mL) was added dropwise. The mixture was refluxed with stirring for 8 h and then cooled to room temperature. The solvent was evaporated under reduced pressure to obtain 10 mL yellowish oily liquid, and 30 mL of dichloromethane was added to precipitate the yellowish solid, which on recrystallization

from methanol gave a bright yellow solid. Yield: 0.76 g, 85.5%; mp: 252 ~ 253 °C. ^1H NMR(DMSO- d_6 , 400 MHz): δ 1.34 (s, 9H, -CH₃), 7.79 (s, 2H, Ar-H), 7.58 ~ 7.61 (m, 2H, Py-H), 8.28, 8.30 (d, J = 8.0 Hz, 2H, Py-H), 8.76 (s, 2H, Py-H), 8.78, 8.79 (d, J = 4.0 Hz, 2H, Py-H), 9.10 (s, 2H, CH=N), 12.34 (s, 1H, -OH), 12.34 (s, 2H, CONH). ESI-MS: m/z = 445.20 [M + H]⁺. Anal. Calcd. (%) for C₂₄H₂₄N₆O₃: C 64.85, H 5.44, N 18.91. Found (%): C 64.89, H 5.49, N 18.84. FT-IR (KBr pellet, ν/cm^{-1}): 3402 (m), 3180 (s), 2961 (s), 2862 (m), 1649 (s), 1617 (s), 1592 (s), 1562 (s), 1459 (m), 1418 (m), 1352 (s), 1304 (s), 1229 (m), 1198 (w), 1159 (s), 1123 (w), 1091 (w), 1066 (w), 1027 (w), 957 (w), 892 (m), 823 (w), 708 (s), 631 (w).

3.2.2. Synthesis of Complexes 1–4

[Cu₄L₂(OCH₃)₂(CH₃OH)₂·2H₂O (1), Cu(Ac)₂·H₂O (39.9 mg, 0.2 mmol) in methanol (40 mL) was added dropwise with stirring to L (44.5 mg, 0.1 mmol) in DMF (5 mL) and the stirring was continued for 2 h. The solution was filtered off and left for slow evaporation at room temperature. Green crystals were obtained after a few days. The crystals were collected by filtration, washed with methanol, and dried to give complex 1 in a 43% yield. Anal. Calcd. (%) for C₅₂H₆₀Cu₄N₁₂O₁₂: C 48.07, H 4.65, N 12.94; Found (%): C 48.18, H 4.53, N 13.06. FT-IR (KBr pellet, ν/cm^{-1}): 3423 (s), 2957 (s), 1615 (s), 1586 (s), 1549 (m), 1505 (s), 1472 (m), 1411 (w), 1375 (s), 1312 (w), 1226 (m), 1194 (w), 1153 (m), 1080 (m), 1048 (m), 958 (w), 917 (w), 844 (w), 822 (w), 763 (w), 731 (m), 703 (m), 639 (m).

[Zn₂L₂Cl₄]·2H₂O·2CH₃OH (2), ZnCl₂ (13.6 mg, 0.1 mmol) in methanol (40 mL) was added with stirring to L (44.5 mg, 0.1 mmol) in DMF (10 mL) and stirring was continued at room temperature for 3 h. Then the same process was used as for 1. Yield (based on Zn): 38%. Anal. Calcd. (%) for C₅₀H₆₀Zn₂Cl₄N₁₂O₁₀: C 47.60, H 4.79, N 13.32; Found (%): C 47.52, H 4.85, N 13.26. FT-IR (KBr pellet, ν/cm^{-1}): 3434 (m), 3192 (m), 2961 (s), 2865 (m), 1620 (s), 1553 (s), 1519 (s), 1475 (m), 1374 (s), 1316 (s), 1239 (m), 1201 (w), 1161 (m), 1099 (m), 963 (w), 909 (w), 836 (w), 778 (w), 733 (m), 703 (m), 651 (w).

[Hg₂L₂Br₄]·4CH₃OH (3), HgBr₂ (36.0 mg, 0.1 mmol) in methanol (40 mL) was added dropwise with stirring to L (44.5 mg, 0.1 mmol) in DMF (5 mL) and stirring was continued at room temperature for 3 h. Then the same process was used as for 1. Yield (based on Hg): 32%. Anal. Calcd. (%) for C₅₂H₆₄Hg₂Br₄N₁₂O₁₀: C 35.94, H 3.71, N 9.67; Found (%): C 35.81, H 3.62, N 9.79. FT-IR (KBr pellet, ν/cm^{-1}): 3542 (n), 3191 (s), 3025 (m), 2961 (s), 2861 (m), 1655 (s), 1616 (s), 1563 (s), 1460 (m), 1427 (m), 1379 (m), 1351 (s), 1295 (s), 1229 (w), 1197 (w), 1159 (m), 1123 (w), 1091 (w), 1051 (w), 957 (m), 895 (m), 826 (m), 756 (w), 702 (s), 638 (w).

{[CdL₂Cl₂]·4H₂O·4CH₃OH}_n (4), CdCl₂·2.5H₂O (22.8 mg, 0.1 mmol) in methanol (40 mL) was added dropwise with stirring to L (88.8 mg, 0.2 mmol) in DMF (10 mL). Then the same process was used as for 1. Yield (based on Cd): 35%. Anal. Calcd. (%) for C₅₂H₇₂CdCl₂N₁₂O₁₄: C 49.08, H 5.70, N 13.21; Found (%): C 49.18, H 5.60, N 13.31. FT-IR (KBr pellet, ν/cm^{-1}): 3452 (m), 3202 (s), 3038 (s), 2957 (s), 2863 (w), 1659 (s), 1617 (s), 1559 (s), 1471 (m), 1428 (w), 1353 (s), 1289 (s), 1229 (w), 1200 (w), 1159 (m), 1093 (w), 1030 (m), 956 (w), 894 (m), 826 (w), 731 (w), 704 (s), 638 (w).

3.3. Crystallographic Data Collection and Structure Determination

Single-crystal X-ray data of complexes 1–4 were collected using a D8 VENTURE diffractometer (Bruker, Berlin, Germany). Intensities of reflections were measured using Mo K α monochromatized radiation (λ = 0.71 073 Å). Data reductions and absorption corrections were performed by using the SAINT and SADABS programs implemented in the APEX2 software (version 1.2), respectively. The structures were solved by direct methods and refined by full-matrix least squares methods on F^2 using the SHELXTL programs [41,42]. All non-H atoms were refined anisotropically. Hydrogen atoms were generated geometrically with fixed isotropic thermal parameters, and included in the structure factor calculations. Some solvent molecules in the four complexes are disorder and removed by Platon/Squeeze in the APEX2 software (version 1.2). Crystal data and structure refinement parameters are listed in Table 2. Selected bond lengths and angles for

the complexes are listed in Supplementary Materials Table S1. Hydrogen bonding lengths and angles are listed in Supplementary Materials Table S2. CCDC reference numbers: 2041792 for **1**, 2041793 for **2**, 2041794 for **3**, and 2041795 for **4**.

Table 2. Crystal data and structure refinement parameters for complexes **1–4**.

Complex	1	2	3	4
Empirical formula	C ₅₂ H ₅₆ Cu ₄ N ₁₂ O ₁₀	C ₄₈ H ₄₈ Cl ₄ N ₁₂ O ₆ Zn ₂	C ₄₈ H ₄₈ Br ₄ Hg ₂ N ₁₂ O ₆	C ₅₂ H ₆₄ CdC ₁₂ N ₁₂ O ₁₀
Formula weight	1263.24	1161.52	1609.80	1200.45
Temperature/K	273(2)	273(2)	223(2)	223(2)
Crystal system	triclinic	triclinic	triclinic	triclinic
Space group	<i>P</i> $\bar{1}$	<i>P</i> $\bar{1}$	<i>P</i> $\bar{1}$	<i>P</i> $\bar{1}$
<i>a</i> /Å	10.227(6)	9.019(5)	9.2634(6)	8.9706(11)
<i>b</i> /Å	11.498(7)	12.473(7)	12.7672(7)	12.3790(15)
<i>c</i> /Å	13.310(8)	15.450(10)	15.2183(9)	15.0517(18)
α /°	113.636(19)	93.56(2)	92.911(2)	80.276(4)
β /°	90.801(19)	103.431(19)	102.156(2)	83.890(5)
γ /°	102.829(19)	105.544(18)	106.228(2)	76.927(4)
<i>V</i> /Å ³	1388.7(15)	1614.3(16)	1677.81(17)	1600.7(3)
<i>Z</i>	1	1	1	1
<i>D_c</i> /(g·cm ^{−3})	1.511	1.195	1.593	1.245
θ range/°	2.48 ≤ θ ≤ 24.00	2.04 ≤ θ ≤ 25.00	3.27 ≤ θ ≤ 25.00	2.58 ≤ θ ≤ 24.50
Absorption coefficient/mm ^{−1}	1.578	0.957	6.998	0.483
<i>F</i> (000)	648	596	768	622
Reflections collected	26104	32817	29072	28266
Independent reflections	4358	5680	5846	5275
Observed reflections (<i>I</i> > 2σ(<i>I</i>))	2454	4404	5282	4331
Number of parameters	361	329	329	357
Goodness-of-fit on <i>F</i> ²	1.042	1.088	1.053	1.099
Final <i>R</i> indices (<i>I</i> > 2σ(<i>I</i>))	<i>R</i> ₁ = 0.0705, <i>wR</i> ₂ = 0.1701	<i>R</i> ₁ = 0.0459, <i>wR</i> ₂ = 0.1318	<i>R</i> ₁ = 0.0336, <i>wR</i> ₂ = 0.0895	<i>R</i> ₁ = 0.0593, <i>wR</i> ₂ = 0.1319
<i>R</i> indices (all data)	<i>R</i> ₁ = 0.1362, <i>wR</i> ₂ = 0.2020	<i>R</i> ₁ = 0.0608, <i>wR</i> ₂ = 0.1397	<i>R</i> ₁ = 0.0396, <i>wR</i> ₂ = 0.0920	<i>R</i> ₁ = 0.0772, <i>wR</i> ₂ = 0.1403
Largest diff. peak and hole (e Å ^{−3})	0.435, −0.530	0.380, −0.454	1.933, −1.229	0.673, −0.580

4. Conclusions

In summary, we have synthesized and characterized four complexes derived from a bis(pyridylhydrazone) ligand with copper(II), zinc(II), mercury(II) and cadmium(II), respectively. The structural analysis reveals that each copper(II) ion is five-coordinated with a square-pyramidal geometry in the tetranuclear complex **1**. The zinc(II) and mercury(II) ions are four-coordinated with a slightly distorted tetrahedral geometry in the metallamacrocycle **2** or **3**. The cadmium ion is six-coordinated with a distorted octahedral geometry in the 1D looped-chain coordination polymer **4**. It is worth noting that the bis(pyridylhydrazone) compound acts as a tridentate ligand in complex **1**, while acting as a bidentate ligand in complexes **2–4**, which indicates that the nature of the ligands play an important role in the coordination networks. The adsorption measurements for the complexes show that they can be potential materials as the adsorbents of methanol vapor.

Supplementary Materials: The following are available online, Figure S1: ¹H NMR for **L**. Figure S2: MS for **L**. Figure S3: IR spectra for **L** and complexes **1–4**. Table S1: Selected bond lengths and angles (°) for complexes **1–4**. Table S2: Hydrogen bonding lengths and angles for complexes **1–4**.

Author Contributions: H.-J.L. carried out the experiments, R.Y. and D.-M.C. analyzed the experiment data, C.H. and B.-X.Z. analyzed the X-ray structure and wrote the paper. All authors have read and agreed to the published version of the manuscript.

Funding: This research was financially supported by the National Natural Science Foundation of China (21961007), the Development Project of young scientific and technological talents of Guizhou Province (QJH-KY[2021]093) and the “Chun-Hui” Fund of Chinese Ministry of Education ([2019]1383).

Data Availability Statement: The data presented in this study are available on request from the corresponding author.

Conflicts of Interest: The authors declare no conflict of interest.

References

1. Khandar, A.A.; Afkhami, F.A.; Yazdi, S.A.H.; Lipkowski, J.; Dougherty, W.G.; Kassel, W.S.; Prieto, H.R.; Granda, S.G. Synthesis, characterization and crystal structure of Zn(II) and Cd(II) One- and two-dimensional coordination polymers derived from pyridine based schiff base ligand. *J. Inorg. Organomet Polym.* **2015**, *25*, 860–868. [[CrossRef](#)]
2. Afkhami, F.A.; Khandar, A.A.; Mahmoudi, G.; Maniukiewicz, W.; Lipkowski, J.; White, J.M.; Waterman, R.; Granda, S.G.; Zangrando, E.; Bauzá, A.; et al. Synthesis, X-ray characterization, DFT calculations and Hirshfeld surface analysis of Zn(II) and Cd(II) complexes based on isonicotinoylhydrazone ligand. *CrystEngComm* **2016**, *18*, 4587–4596. [[CrossRef](#)]
3. Bhaskar, R.S.; Ladole, C.A.; Salunkhe, N.G.; Barabde, J.M.; Aswar, A.S. Synthesis, characterization and antimicrobial studies of novel ONO donor hydrazone Schiff base complexes with some divalent metal (II) ions. *Arab. J. Chem.* **2020**, *13*, 6559–6567. [[CrossRef](#)]
4. Singh, R.K.; Singh, A.K.; Siddiqui, S.; Arshad, M.; Jafri, A. Synthesis, molecular structure, spectral analysis and cytotoxic activity of two new aroylhydrazones. *J. Mol. Struct.* **2017**, *1135*, 82–97. [[CrossRef](#)]
5. Çınarlı, M.; Ataol, Ç.Y.; Çınarlı, E.; Idil, Ö. Synthesis, characterization, biological, X-ray diffraction analysis and computational chemistry studies of new 2-acetylpyridine derivative hydrazone and its Zn(II) complex. *J. Mol. Struct.* **2020**, *1213*, 128152. [[CrossRef](#)]
6. Wang, L.; Guo, D.G.; Wang, Y.Y.; Zheng, C.Z. 4-Hydroxy-3-methoxy-benzaldehyde series aroyl hydrazones: Synthesis, thermostability and antimicrobial activities. *RSC Adv.* **2014**, *4*, 58895–58901. [[CrossRef](#)]
7. Kendel, A.; Miljanić, S.; Kontrec, D.; Soldin, Ž.; Galić, N. Copper(II) complexes of aroylhydrazones: Preparation and structural characterization. *J. Mol. Struct.* **2020**, *1207*, 127783. [[CrossRef](#)]
8. Kamatchi, T.S.; Subarkhan, M.K.M.; Ramesh, R.; Wang, H.X.; Mafecki, J.G. Investigation into antiproliferative activity and apoptosis mechanism of new arene Ru(II) carbazole-based hydrazone complexes. *Dalton Trans.* **2020**, *49*, 11385–11395. [[CrossRef](#)]
9. Abouzayed, F.I.; Emam, S.M.; Abouel-Enein, S.A. Synthesis, characterization and biological activity of nano-sized Co(II), Ni(II), Cu(II), Pd(II) and Ru(III) complexes of tetradentate hydrazone ligand. *J. Mol. Struct.* **2020**, *1216*, 128314. [[CrossRef](#)]
10. Santiago, P.H.O.; Santiago, M.B.; Martins, C.H.G.; Gatto, C.C. Copper(II) and zinc(II) complexes with Hydrazone: Synthesis, crystal structure, Hirshfeld surface and antibacterial activity. *Inorg. Chim. Acta* **2020**, *508*, 119632. [[CrossRef](#)]
11. Xu, J.; Zhou, T.; Xu, Z.Q.; Gu, X.N.; Wu, W.N.; Chen, H.; Wang, Y.; Jia, L.; Zhu, T.F.; Chen, R.H. Synthesis, crystal structures and antitumor activities of copper(II) complexes with a 2-acetylpyridine isonicotinoyl hydrazone ligand. *J. Mol. Struct.* **2017**, *1128*, 448–454. [[CrossRef](#)]
12. Yang, Q.Y.; Cao, Q.Q.; Qin, Q.P.; Deng, C.X.; Liang, H.; Chen, Z.F. Syntheses, crystal structures, and antitumor activities of Copper(II) and Nickel(II) complexes with 2-((2-(Pyridin-2-yl)hydrazono)methyl)quinolin-8-ol. *Int. J. Mol. Sci.* **2018**, *19*, 1874. [[CrossRef](#)] [[PubMed](#)]
13. Santos, A.F.; Ferreira, I.P.; Pinheiro, C.B.; Santos, V.G.; Lopes, M.T.P.; Teixeira, L.R.; Rocha, W.R.; Rodrigues, G.L.S.; Beraldo, H. [Ag(L)NO₃] complexes with 2-Benzoylpyridine-derived Hydrazones: Cytotoxic activity and interaction with biomolecules. *ACS Omega* **2018**, *3*, 7027–7035. [[CrossRef](#)] [[PubMed](#)]
14. Ramachandran, E.; Gandin, V.; Bertani, R.; Sgarbossa, P.; Natarajan, K.; Bhuvanesh, N.S.P.; Venzo, A.; Zoleo, A.; Glisenti, A.; Dolmella, A.; et al. Synthesis, characterization and cytotoxic activity of novel copper(II) complexes with aroylhydrazone derivatives of 2-Oxo-1,2-dihydrobenzo[h] quinoline-3-carbaldehyde. *J. Inorg. Biochem.* **2018**, *182*, 18–28. [[CrossRef](#)]
15. Bergamini, F.R.G.; Nunes, J.H.B.; Carvalho, M.A.; Ribeiro, M.A.; Paiva, P.P.; Banzato, T.P.; Ruiz, A.L.T.G.; Carvalho, J.E.; Lustri, W.R.; Martins, D.O.T.A.; et al. Polynuclear copper(II) complexes with nalidixic acid hydrazones: Antiproliferative activity and selectivity assessment over a panel of tumor cells. *Inorg. Chim. Acta* **2019**, *484*, 491–502. [[CrossRef](#)]
16. Rocha, C.S.; Filho, L.F.O.B.; Souza, A.E.; Diniz, R.; Denadai, A.M.L.; Beraldo, H.; Teixeira, L.R. Structural studies and investigation on the antifungal activity of silver(I) complexes with 5-nitrofurane-derived hydrazones. *Polyhedron* **2019**, *170*, 723–730. [[CrossRef](#)]
17. Bakale, R.P.; Naik, G.N.; Machakanur, S.S.; Mangannavar, C.V.; Muchchandi, I.S.; Gudasi, K.B. Structural characterization and antimicrobial activities of transition metal complexes of a hydrazone ligand. *J. Mol. Struct.* **2018**, *1154*, 92–99. [[CrossRef](#)]
18. Mahmoud, A.G.; Silva, M.F.C.G.; Mahmudov, K.T.; Pompeiro, A.J.L. Arylhydrazone ligands as Cu-protectors and -catalysis promoters in the azide-alkyne cycloaddition reaction. *Dalton Trans.* **2019**, *48*, 1774–1785. [[CrossRef](#)]
19. Wu, Y.; Gu, Z.J.; Luo, W.; Wu, L.; Li, Y.L.; Xie, B.; Zuo, L.K. Crystal structure, luminescent sensing and photocatalytic activity of a multifunctional hydrazone-based zinc(II) coordination polymer. *Transit. Metal Chem.* **2018**, *43*, 673–681. [[CrossRef](#)]
20. Chen, D.M.; Wu, X.F.; Liu, Y.J.; Huang, C.; Zhu, B.X. Synthesis, crystal structures and vapor adsorption properties of Hg(II) and Cd(II) coordination polymers derived from two hydrazone Schiff base ligands. *Inorg. Chim. Acta* **2019**, *494*, 181–186. [[CrossRef](#)]

21. Matoga, D.; Szklarzewicz, J.; Nitek, W. Effect of ligand substituents on supramolecular self-assembly and electrochemical properties of copper(II) complexes with benzoylhydrazones: X-ray crystal structures and cyclic voltammetry. *Polyhedron* **2012**, *36*, 120–126. [[CrossRef](#)]
22. Chelike, D.K.; Alagumalai, A.; Muthukumar, V.R.; Thangavelu, S.A.G.; Krishnamoorthy, A. Tunable yellow–green emitting cyclotriphosphazene appended phenothiazine hydrazone hybrid material: Synthesis, characterisation, photophysical and electrochemical studies. *New J. Chem.* **2020**, *44*, 13401–13414. [[CrossRef](#)]
23. Sathiyakumar, S.; Selvam, P.; Hakkim, F.L.; Srinivasan, K.; Harrison, W.T.A. Mechanochemical syntheses, crystal structures, and photo-luminescent properties of a new hydrazone and its nickel and cadmium complexes. *J. Coord. Chem.* **2018**, *71*, 3521–3533. [[CrossRef](#)]
24. Sennappan, M.; Krishna, P.M.; Hosamani, A.A.; Krishna, R.H. Synthesis, characterization, nucleic acid interactions and photoluminescent properties of methaniminium hydrazone Schiff base and its Mn(II), Co(II), Ni(II), Cu(II), Zn(II) and Cd(II) complexes. *J. Mol. Struct.* **2018**, *1164*, 271–279. [[CrossRef](#)]
25. Warr, R.J.; Willis, A.C.; Wild, S.B. Inorganic asymmetric synthesis: Diastereoselective syntheses of Monoand dinuclear complexes containing octahedral, two-bladed propeller, Bis(pyridine-2-aldehyde 2'-pyridylhydrazone)iron(II) Stereocenters. *Inorg. Chem.* **2008**, *47*, 9351–9362. [[CrossRef](#)] [[PubMed](#)]
26. Nakamura, T.; Kimura, H.; Okuhara, T.; Yamamura, M.; Nabeshima, T. A Hierarchical Self-Assembly System Built Up from Preorganized Tripodal Helical Metal Complexes. *J. Am. Chem. Soc.* **2016**, *138*, 794–797. [[CrossRef](#)] [[PubMed](#)]
27. Chaur, M.N.; Collado, D.; Lehn, J.M. Configurational and constitutional information storage: Multiple dynamics in systems based on Pyridyl and Acyl Hydrazones. *Chem. Eur. J.* **2011**, *17*, 248–258. [[CrossRef](#)]
28. Nesterova, O.V.; Chygorin, E.N.; Kokozay, V.N.; Bon, V.V.; Omelchenko, I.V.; Shishkin, O.V.; Titiš, J.; Boča, R.; Pombeiro, A.J.L.; Ozarowski, A. Magnetic, high-field EPR studies and catalytic activity of Schiff base tetranuclear CuII2 FeIII2 complexes obtained by direct synthesis. *Dalton Trans.* **2013**, *42*, 16909–16919. [[CrossRef](#)]
29. Chen, L.D.; Huo, H.L.; Ma, L.L.; Jiang, Y.; Xie, J.Y.; Wang, J. Nickel complexes based on Salicylaldehyde-imine ligands: Synthesis, characterization and catalytic oligomerization of Ethylene. *Chem. Res. Chin. Univ.* **2018**, *34*, 945–951. [[CrossRef](#)]
30. Sarkar, R.; Hens, A.; Rajak, K.K. Synthesis, characterization and DFT study of oxorhenium(V) complexes incorporating quinoline based tridentate ligands. *RSC Adv.* **2015**, *5*, 15084–15095. [[CrossRef](#)]
31. Andrežalová, L.; Plšíková, J.; Janocková, J.; Koňariková, K.; Žitňanová, I.; Kohútová, M.; Kožurková, M. DNA/BSA binding ability and genotoxic effect of mono- and binuclear copper (II) complexes containing a Schiff base derived from salicylaldehyde and D, L-glutamic acid. *J. Organomet. Chem.* **2017**, *827*, 67–77. [[CrossRef](#)]
32. Addison, A.W.; Rao, T.N.; Reedijk, J.; van Rijn, J.; Verschoor, G.C. Synthesis, structure, and spectroscopic properties of copper(II) compounds containing nitrogen–sulphur donor ligands; the crystal and molecular structure of aqua[1,7-bis(N-methylbenzimidazol-2'-yl)-2,6-dithiaheptane]copper(II) perchlorate. *J. Chem. Soc. Dalton Trans.* **1984**, *3*, 1349–1356. [[CrossRef](#)]
33. Rodríguez-Hermida, S.; Wende, C.; Lago, A.B.; Carballo, R.; Kulak, N.; Vázquez-López, E.M. Reaction of a Bis(benzoylhydrazone) with Copper(II): Complex formation, hydroxylation, and DNA cleavage activity. *Eur. J. Inorg. Chem.* **2013**, *2013*, 5843–5853. [[CrossRef](#)]
34. Özdemir, Ü.Ö.; Aktan, E.; Ilbiz, F.; Gündüzalp, A.B.; Özbek, N.; Sarı, M.; Çelik, Ö.; Saydam, S. Characterization, antibacterial, anticarbonic anhydrase II isoenzyme, anticancer, electrochemical and computational studies of sulfonic acid hydrazide derivative and its Cu(II) complex. *Inorg. Chim. Acta* **2014**, *413*, 194–203. [[CrossRef](#)]
35. Gupta, R.; Mukherjee, S.; Mukherjee, R. Synthesis, magnetism, ¹H NMR and redox activity of dicopper(II) complexes having a discrete {Cu₂(μ-phenoxide)₂}²⁺ unit supported by a non-macrocyclic ligand environment. Crystal structure of [Cu₂(L)₂(OClO₃)₂] [HL = 4-methyl-2,6-bis(pyrazol-1-ylmethyl)-phenol]. *J. Chem. Soc. Dalton Trans.* **1999**, *4*, 4025–4030.
36. Yang, L.; Powell, D.R.; Houser, R.P. Structural variation in copper(I) complexes with pyridylmethylamide ligands: Structural analysis with a new four-coordinate geometry index, τ₄. *Dalton Trans.* **2007**, *4*, 955–964. [[CrossRef](#)]
37. Hain, M.S.; Fukuda, Y.; Ramírez, C.R.; Winer, B.Y.; Winslow, S.E.; Pike, R.D.; Bebout, D.C. Staging bonding between group 12 metal ions and neutral selenium donors: Intermolecular interactions of mixed N, Se Donor ligands and anions. *Cryst. Growth Des.* **2014**, *14*, 6497–6507. [[CrossRef](#)]
38. Liu, Y.J.; Chen, Y.T.; Chen, M.Z.; Mo, X.J.; Huang, C.; Chen, D.M.; Zhu, B.X. Self-discriminating and counteranion-controlled self-assembly: Two heterochiral Cd(II) coordination polymers based on a racemic bis(pyridyl) ligand. *Inorg. Chim. Acta* **2020**, *510*, 119702. [[CrossRef](#)]
39. Huang, C.; Luo, X.; Zhai, J.; Chen, Y.; Chen, D.M.; Zhu, B.X. [2+2] or [4+4] metallamacrocyclic: Synthesis and crystal structures of Hg(II) complexes derived from two flexible bis(pyridylurea) ligands. *Polyhedron* **2019**, *165*, 111–115. [[CrossRef](#)]
40. Li, Y.H.; Zhao, Y.R.; Chan, W.H.; Wang, Y.J.; You, Q.H.; Liu, C.H.; Zheng, J.; Li, J.S.; Yang, S.; Yang, R.H. Selective tracking of Lysosomal Cu²⁺ ions using simultaneous target- and location-activated fluorescent nanoprobes. *Anal. Chem.* **2015**, *87*, 584–591. [[CrossRef](#)]
41. Sheldrick, G.M. Crystal structure refinement with SHELXL. *Acta Cryst. C* **2015**, *71*, 3–8. [[CrossRef](#)] [[PubMed](#)]
42. Dolomanov, O.V.; Bourhis, L.J.; Gildea, R.J.; Howard, J.A.K.; Puschmann, H. OLEX2: A Complete Structure Solution, Refinement and Analysis Program. *J. Appl. Cryst.* **2009**, *42*, 339–341. [[CrossRef](#)]